

1                    **Kinetic and equilibrium modelling of MTBE**  
2  
3  
4                    **(Methyl tert-butyl ether) adsorption on ZSM-5**  
5  
6  
7                    **zeolite: Batch and column studies**  
8  
9

10  
11                    *Yunhui Zhang<sup>a\*</sup>; Fei Jin<sup>b</sup>; Zhengtao Shen<sup>c</sup>; Rod Lynch<sup>a</sup>; Abir Al-Tabbaa<sup>a</sup>*  
12  
13

14  
15                    <sup>a</sup>Department of Engineering, University of Cambridge, Cambridge, CB2 1PZ, United Kingdom

16                    <sup>b</sup>School of Engineering, University of Glasgow Singapore, 138683, Singapore

17  
18                    <sup>c</sup>Department of Earth and Atmospheric Sciences, University of Alberta, T6G 2E3, Canada  
19  
20  
21  
22  
23  
24  
25  
26  
27  
28  
29

30                    **AUTHOR INFORMATION**  
31

32                    **\*Corresponding Author**  
33

34                    Tel: +44- (0) 7821464199  
35

36                    E-mail address: yz485@cam.ac.uk.  
37  
38  
39  
40  
41  
42  
43  
44  
45  
46  
47  
48  
49  
50  
51  
52  
53  
54  
55  
56  
57  
58  
59  
60  
61  
62  
63  
64  
65

## Abstract

The intensive use of methyl tert-butyl ether (MTBE) as a gasoline additive has resulted in serious environmental problems due to its high solubility, volatility and recalcitrance. The feasibility of permeable reactive barriers (PRBs) with ZSM-5 type zeolite as a reactive medium was explored for MTBE contaminated groundwater remediation. Batch adsorption studies showed that the MTBE adsorption onto ZSM-5 follows the Langmuir model and obeys the pseudo-second-order model with an adsorption capacity of  $53.55 \text{ mg}\cdot\text{g}^{-1}$ . The adsorption process reached equilibrium within 24 h, and MTBE was barely desorbed with initial MTBE concentration of  $300 \text{ mg}\cdot\text{L}^{-1}$ . The mass transfer process is found to be primarily controlled by pore diffusion for MTBE concentrations from 100 to  $600 \text{ mg}\cdot\text{L}^{-1}$ . pH has little effect on the maximum adsorption capacity in the pH range of 2-10, while the presence of nickel reduces the capacity with Ni concentrations of  $2.5\text{-}25 \text{ mg}\cdot\text{L}^{-1}$ . In fixed-bed column tests, the Dose-Response model fits the breakthrough curve well, showing a saturation time of  $\sim 320$  min and a removal capacity of  $\sim 18.71 \text{ mg}\cdot\text{g}^{-1}$  under the conditions of this study. Therefore, ZSM-5 is an extremely effective adsorbent for MTBE removal and has a huge potential to be used as a reactive medium in PRBs.

**Key words:** MTBE, ZSM-5 zeolite, batch adsorption, mass transfer mechanism, fixed-bed column test

## 1. Introduction

1  
2 Methyl tert-butyl ether (MTBE) was a widely used gasoline additive. Although it has been  
3  
4 banned in some countries, the residual contamination exists due to fugitive emissions from  
5  
6 petrol refineries and petrol filling stations, emissions from vehicles, petrol spills and leaking  
7  
8 storage tanks [1]. The last report of UST (Underground Storage Tank) performance measures  
9  
10 indicated that approximately 13.6% of UST releases remained to be cleaned up in the year of  
11  
12 2015 [2]. In addition, it is reported that tanks did not pass the leakage tests in some regions [3]  
13  
14 and probably affected the aquifers or groundwater where the remediation has always been  
15  
16 considered to be difficult, expensive and slow [4]. Considering that groundwater is an  
17  
18 important source of water supply worldwide, especially for where there is a shortage of  
19  
20 surface water or lakes, groundwater remediation is of great significance for water supply and  
21  
22 human health worldwide.  
23  
24  
25  
26  
27  
28  
29  
30

31  
32 MTBE has an unpleasant odour and harmful effects on the respiratory and nerve systems of  
33  
34 living things although its carcinogenesis remains unclear [5]. MTBE pollution in the  
35  
36 environment mainly exists in groundwater and aquifers rather than in surface water and soil  
37  
38 due to its high solubility, volatility and recalcitrance and has received increasing attention  
39  
40 worldwide [6].  
41  
42  
43  
44  
45

46  
47 MTBE is found to be resistant to chemical and biological degradations [7] and therefore  
48  
49 immobilisation may be a more suitable treatment. In-situ technologies have attracted  
50  
51 increased attention in terms of groundwater and aquifer remediation of MTBE ascribed to  
52  
53 their low costs and simple operation over conventional technologies such as pump and treat.  
54  
55 Permeable reactive barriers (PRBs) are one of the most promising in-situ treatments [8].  
56  
57 Barriers filled with reactive materials are constructed across the flow path of a contaminant  
58  
59  
60  
61  
62  
63  
64  
65

1  
2  
3  
4  
5  
6  
7  
8  
9  
10  
11  
12  
13  
14  
15  
16  
17  
18  
19  
20  
21  
22  
23  
24  
25  
26  
27  
28  
29  
30  
31  
32  
33  
34  
35  
36  
37  
38  
39  
40  
41  
42  
43  
44  
45  
46  
47  
48  
49  
50  
51  
52  
53  
54  
55  
56  
57  
58  
59  
60  
61  
62  
63  
64  
65

plume [9]. As the fluid moves through the PRBs, contaminants are degraded or trapped by reactive materials through physical, chemical and/or biological processes.

The reactive medium is the key component of PRBs and its selection is dependent on the nature of the target contaminants and hydro-geological site conditions. ZSM-5, a high-silica MFI type zeolite, has been found to be effective for MTBE adsorption due to its hydrophobicity and suitable pore size [10,11]. Although the use of natural or modified zeolites has been extensively studied [12,13] due to their good adsorptivity, stability and renewability, research on the use of ZSM-5 as the reactive material in PRBs is limited. Vignola et al. [14,15] utilised ZSM-5 for in-situ PRBs located close to a coastal refinery to remediate MTBE and hydrocarbons contaminated groundwater and the results showed that MTBE was reduced to under 10 µg/L for about 100 days. Faisal and Hmood [16] used ZSM-5 in laboratory-scale PRBs to remove cadmium from a contaminated shallow aquifer and the PRBs started to saturate after ~120 h under conditions tested. For the design of PRBs, it is crucial to figure out the detailed adsorption process of MTBE onto ZSM-5, which necessitates an understanding of kinetics, isotherms, the rate-limiting step, influencing factors and the desorption behaviour [17]. However, to date, most studies have focused on the relationship between the properties of ZSM-5 and its adsorption capacities for MTBE, and there is a lack of research on the detailed adsorption and desorption features.

This work aims to explore the detailed mass transfer mechanisms, adsorption and desorption features of ZSM-5 and to examine its feasibility in PRBs for MTBE removal. Adsorption kinetics, isotherms and desorption kinetics are presented and the diffusion parameters were modelled to assess the rate-limiting step of the entire batch adsorption process. Due to the fact that the real groundwater conditions, such as pH and the existence of heavy metals, are

complex and may have an effect on MTBE adsorption, different influencing factors, such as initial solution pH, solid/liquid ratio and the presence of nickel ions, are explored in this study. In addition, fixed-bed column experiments are performed to evaluate the effectiveness of ZSM-5 as a reactive medium in PRBs.

## 2. Materials and methods

### 2.1 Materials

MTBE and ZSM-5 were purchased from Fisher Scientific and Acros Organics, respectively.

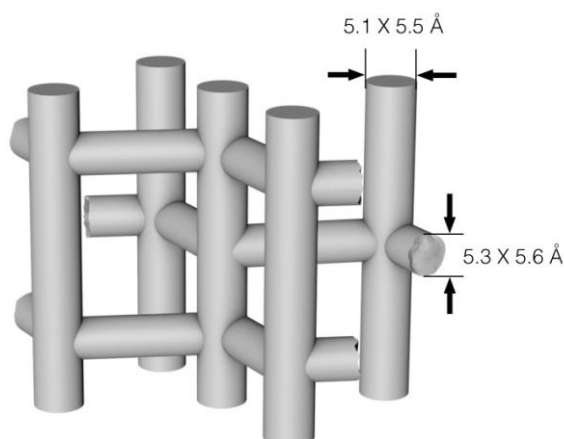
The physicochemical properties of ZSM-5 were obtained from the supplier and are given in

Table 1. **Figure 1 was adapted [18] and presented the molecular structure and dimensions of ZSM-5. There are two pore systems in ZSM-5, one consisting of zig-zag channels of the near-circular cross-section and another consisting of straight channels of the elliptical shape.**

Other chemicals used (HCl, NaOH, NiSO<sub>4</sub>·6H<sub>2</sub>O) were obtained from Fisher Scientific with A.R. grade.

Table 1 The physicochemical properties of ZSM-5

Surface area (m <sup>2</sup> ·g <sup>-1</sup> )	Pore size (Å)	Particle size (μm)	SiO <sub>2</sub> /Al <sub>2</sub> O <sub>3</sub>	pH	CEC (cmol·kg <sup>-1</sup> )
400	5.3x5.6; 5.1x5.5	2-8	469	4.14	1.808



## Figure 1 Molecular structure and dimensions of ZSM-5 [18]

### 2.2 Batch adsorption studies

#### 2.2.1 Kinetic study

Batch kinetic studies were carried out by adding 0.1 g of ZSM-5 into 60 mL small air-tight glass bottles with minimum headspace containing 20 mL MTBE solutions with different concentrations (100, 150, 300 or 600 mg·L<sup>-1</sup>) to avoid the evaporative loss of MTBE [19].

The agitation speed was kept constant at 200 rpm in a shaker for a pre-determined time before filtration using a 0.45 µm glass fiber filter. The shaking time was set at 5 min, 10 min, 20 min, 30 min, 3 h, 6 h, 12 h, 24 h, 48 h, 72 h and 96 h.

#### 2.2.2 Equilibrium study

To study the adsorption isotherm of MTBE onto ZSM-5, 0.1 g of ZSM-5 was added to 20 mL solutions containing different MTBE concentrations (20, 60, 100, 150, 300, 600 and 800 mg·L<sup>-1</sup>). From the kinetic study, it was found that 24 h was required to reach equilibrium.

The following influencing factors were considered:

- (1) The effect of solution pH was examined by varying the initial pH of the solutions from pH 2 to 10. The pH was adjusted using 0.1 M HCl or 0.1 M NaOH. The initial MTBE concentration was fixed at 300 mg·L<sup>-1</sup> with ZSM-5 dosage of 0.1 g/20 mL.
- (2) The effect of solid/liquid ratio was evaluated by adding different amounts of ZSM-5 (0.02, 0.05, 0.08, 0.1, 0.2 and 0.3 g) to 20 mL of 300 mg·L<sup>-1</sup> MTBE solutions.
- (3) The effect of the existence of nickel ions was examined by mixing 0.1 g ZSM-5 with 300 mg·L<sup>-1</sup> MTBE solutions containing various concentrations of Ni (0, 2.5 and 25 mg·L<sup>-1</sup>) at pH = 7.

1 In addition, after the batch adsorption experiments for 24 h (with initial MTBE concentration  
2 of 300 mg·L<sup>-1</sup> and ZSM-5 dosage of 0.1 g). The samples were centrifuged and the  
3 supernatant was decanted. Desorption kinetic experiments were performed by the addition of  
4 20 mL deionized water with a stirring speed of 200 rpm for various time periods (same with  
5 those of adsorption kinetic tests).  
6  
7  
8  
9  
10

### 11 2.3 Fixed-bed column tests

12 Fixed-bed column tests were conducted on a laboratory scale to simulate the application of  
13 ZSM-5 in PRBs for MTBE removal. The tests were performed using 2 cm inner diameter and  
14 10 cm high Pyrex glass columns. Columns were packed with a mixture of ZSM-5 (5%) and  
15 model sandy soil. Model soil samples were made by mixing 92% sand with 3% clay and 5%  
16 slit represented by kaolin and silica flour, respectively. This model soil is classified as sand  
17 [20]. The water content is 10% and the density is about 2 g·cm<sup>-3</sup>. The porosities of model soil  
18 and the mixture are 32.41% and 31.63%, respectively. The total bed length is 9 cm and initial  
19 MTBE concentration is 300 mg·L<sup>-1</sup>. The flow rate is kept constant at 2 mL·min<sup>-1</sup>. Aqueous  
20 samples were collected at regular intervals and analysed for MTBE concentrations  
21 throughout the test period. From a practical point of view, the saturation time,  $t_s$ , is  
22 established when the concentration in the effluent is higher than 90% of the inlet  
23 concentration [21]. The breakthrough time here,  $t_b$ , is established when the MTBE  
24 concentration in the effluent reaches 50% of the inlet concentration.  
25  
26  
27  
28  
29  
30  
31  
32  
33  
34  
35  
36  
37  
38  
39  
40  
41  
42  
43  
44  
45  
46  
47  
48  
49

### 50 2.4 Analytical methods

51 MTBE was analyzed using a gas chromatograph (Agilent 6850 Series) with a flame  
52 ionisation detector (GC-FID) by an ambient headspace technique at 20°C as used in our  
53 previous study [22]. Each headspace sample was measured in triplicate. Blank experiments  
54 were carried out under identical conditions with adsorption experiments for all the MTBE  
55  
56  
57  
58  
59  
60  
61  
62  
63  
64  
65

1 concentrations and showed negligible influence of the MTBE volatility on the test results.  
2 The concentration of Ni<sup>2+</sup> was measured by inductively coupled plasma-optical emission  
3 spectrometry (ICP-OES) (Perkin-Elmer, 7000DV) after dilution and acidification. OriginPro  
4 8.5 software was used to perform data fitting and modelling and output fitting values,  
5 standard errors, correlation coefficient (R<sup>2</sup>) and Akaike information criterion (AIC) values.  
6  
7 The AIC and R<sup>2</sup> values were used in this study to compare predictions with the experimental  
8 data and find out the best fitting model. AIC is an estimator of the relative quality  
9 of statistical models for a given set of data and provides a means for model selection. The  
10 model with higher R<sup>2</sup> and lower AIC values is preferred.  
11  
12  
13  
14  
15  
16  
17  
18  
19  
20  
21  
22  
23

### 24 **3. Results and discussion**

#### 25 **3.1 Adsorption kinetics**

26 The pseudo-first-order and pseudo-second-order models were used to describe the kinetics of  
27 MTBE adsorption onto ZSM-5. The fitting of the experimental kinetics data is presented in  
28 Figure 2 and Table 2. Where q<sub>e</sub> and q<sub>t</sub> are the amount of adsorbate adsorbed at equilibrium  
29 and time t (mg·g<sup>-1</sup>), respectively, k<sub>1</sub> and k<sub>2</sub> are the rate constants of pseudo-first-order  
30 adsorption (h<sup>-1</sup>) and pseudo-second-order adsorption (g·mg<sup>-1</sup>·s<sup>-1</sup>), respectively.  
31  
32  
33  
34  
35  
36  
37  
38  
39  
40  
41  
42  
43  
44  
45  
46  
47  
48  
49  
50  
51  
52  
53  
54  
55  
56  
57  
58  
59  
60  
61  
62  
63  
64  
65



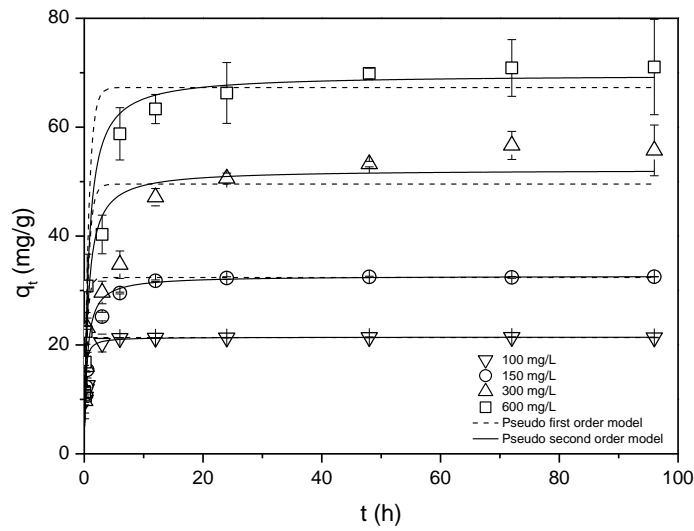


Figure 2 The fitting of pseudo-first-order and pseudo-second-order models for MTBE adsorption onto ZSM-5 at different initial concentrations

Table 2 Kinetics model parameters for MTBE adsorption onto ZSM-5 at different MTBE concentrations

Models	Equations	Parameters	Initial MTBE concentration (mg·L <sup>-1</sup> )			
			100	150	300	600
Pseudo-first-order	$q_t = q_e(1 - e^{-k_1 t})$	$q_e$ (mg·g <sup>-1</sup> )	21.35±0.10	32.40±0.20	49.55±2.94	67.29±2.40
		$k_1$ (h <sup>-1</sup> )	5.57±0.74	2.35±0.80	1.59±0.11	1.40±0.38
		AIC	43.59	51.04	50.95	29.98
		R <sup>2</sup>	0.94	0.84	0.95	0.92
			10	20	94	0
Pseudo-second-order	$q_t = \frac{q_e^2 k_2 t}{1 + q_e k_2 t}$	$q_e$ (mg·g <sup>-1</sup> )	21.44±0.07	32.68±0.09	52.19±1.56	69.64±1.68
		$k_2$ (g·mg <sup>-1</sup> ·h <sup>-1</sup> )	0.38±0.04	0.067±0.01	0.03±0.00	0.021±0.00
		$t_{1/2}$ (s)	437.23	1644.07	2090.22	2461.75
		AIC	34.44	31.41	35.91	20.22
		R <sup>2</sup>	0.97	0.97	0.99	0.97
			07	09	56	8

1  
2  
3  
4  
5  
6  
7  
8  
9  
10  
11  
12  
13  
14  
15  
16  
17  
18  
19  
20  
21  
22  
23  
24  
25  
26  
27  
28  
29  
30  
31  
32  
33  
34  
35  
36  
37  
38  
39  
40  
41  
42  
43  
44  
45  
46  
47  
48  
49  
50  
51  
52  
53  
54  
55  
56  
57  
58  
59  
60  
61  
62  
63  
64  
65

It was shown in Figure 2 that the adsorption of MTBE onto ZSM-5 was found to be rapid at the initial period and then plateaued with the increasing contact time. It was found that 24 h was deemed sufficient to ensure equilibrium for all the concentrations, and the equilibrium time increased with the increase of the initial MTBE concentration. From Table 2, it was found that the pseudo-second-order model was the best at all concentrations for MTBE adsorption onto ZSM-5, indicating chemisorption [23]. The amount of adsorbed MTBE increased from 21.44 mg·g<sup>-1</sup> to 69.64 mg·g<sup>-1</sup> by increasing the initial MTBE concentration from 100 mg·L<sup>-1</sup> to 600 mg·L<sup>-1</sup>.

In addition, as shown in Table 2, the half-adsorption time ( $t_{1/2}$ ) [24] was applied to further describe the adsorption equilibrium time of MTBE onto ZSM-5.  $t_{1/2}$ , the time required for the ZSM-5 to uptake half of the amount adsorbed at equilibrium, is typically considered as a measure of the rate of adsorption. The increase of  $t_{1/2}$  values (from 437.23 s<sup>-1</sup> to 2461.75 s<sup>-1</sup>) indicated the increase of adsorption rate with the increase of MTBE concentration from 100 mg·L<sup>-1</sup> to 600 mg·L<sup>-1</sup>.

### 3.2 Adsorption isotherms

As shown in Figure 3, the experimental data were fitted with the widely used isotherm models for solid-liquid adsorption by nonlinear regression, i.e. Langmuir, Freundlich, modified form of BET [25], Sips, Dubinin-Radushkevich and Temkin models [26]. The isotherm equations, regression analysis and model parameters are given in Table 3. For the Langmuir model,  $Q_0$  is the maximum adsorption capacity (mg·g<sup>-1</sup>),  $b$  is the rate of adsorption (L·mg<sup>-1</sup>);  $C_e$  is the MTBE equilibrium concentration (mg·L<sup>-1</sup>),  $R_L$  is the equilibrium parameter to describe the essential characteristics of Langmuir isotherm,  $C_0$  is the initial MTBE concentration (mg·L<sup>-1</sup>). For the Freundlich model,  $K_F$  is the adsorption capacity of the

adsorbent ( $\text{mg}\cdot\text{g}^{-1}$ );  $1/n$  ranging between 0 and 1 is a measure of adsorption intensity or surface heterogeneity, and the surface of the adsorbent is more heterogeneous if its value is closer to zero. For the BET model,  $K_B$  and  $K_L$  are the equilibrium constants of adsorption for the first and upper layers ( $\text{L}\cdot\text{mg}^{-1}$ ), respectively,  $q_m$  is the theoretical isotherm saturation capacity ( $\text{mg}\cdot\text{g}^{-1}$ ). For the Sips model,  $K_s$  is the equilibrium constant ( $\text{L}\cdot\text{mg}^{-1}$ ). For the Dubinin-Radushkevich model,  $K_D$  is the mean free energy of sorption per molecule of the sorbate when it is transferred to the surface of the solid from infinity in the solution ( $\text{mol}^2\cdot\text{kJ}^2$ ),  $R$  ( $8.314 \text{ J}\cdot\text{mol}^{-1}\cdot\text{K}^{-1}$ ) is the universal gas constant and  $T$  (K) is the solution temperature. For the Temkin model,  $RT/b_T=B$  ( $\text{J}\cdot\text{mol}^{-1}$ ), which is the Temkin constant related to the heat of sorption,  $A_T$  is the equilibrium binding constant corresponding to the maximum binding energy ( $\text{L}\cdot\text{g}^{-1}$ ).

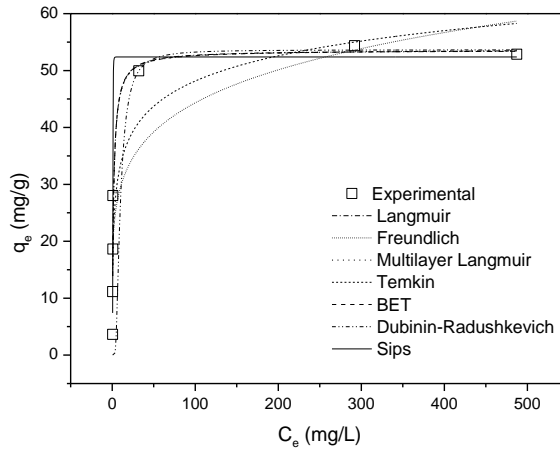


Figure 3 Isotherm plots for MTBE adsorption onto ZSM-5

Table 3 Isotherm model parameters for MTBE adsorption on ZSM-5

Models	Equations	Parameters	
Langmuir	$q_e = \frac{Q_0 b C_e}{1 + b C_e}$	$Q_0$ ( $\text{mg}\cdot\text{g}^{-1}$ )	$53.55\pm 4.07$
		$b$ ( $\text{L}\cdot\text{mg}^{-1}$ )	$0.62\pm 0.20$
	$R_L = \frac{1}{1 + b C_0}$	$R_L$	0.002
		AIC	38.34

		$R^2$	0.90
Freundlich	$q_e = C_e^{\frac{1}{n}} K_F$	$K_F (mg \cdot g^{-1})$	19.60±4.91
		1/n	0.18±0.65
		AIC	44.53
		$R^2$	0.76
BET	$q_e = q_m \frac{K_B C_e}{(1 - K_L C_e)(1 - K_L C_e + K_B C_e)}$	$q_m (mg \cdot g^{-1})$	53.42±8.61
		$K_L (L \cdot mg^{-1})$	8.35×10 <sup>-6</sup> ±4.66×10 <sup>-4</sup>
		$K_B (L \cdot mg^{-1})$	0.62±0.27
		AIC	52.34
		$R^2$	0.87
Sips	$q_e = Q_0 \frac{K_S C_e^{\frac{1}{n}}}{1 + K_S C_e^{\frac{1}{n}}}$	$K_S (L \cdot mg^{-1})$	2.57±1.48
		$Q_0 (mg \cdot g^{-1})$	52.39±2.62
		$N$	0.21±0.07
		AIC	45.27
		$R^2$	0.95
Dubinin-Radushkevich	$q_e = q_m \exp\left(-K_D \left(RT \ln\left(1 + \frac{1}{C_e}\right)\right)^2\right)$	$q_m (mg \cdot g^{-1})$	53.64±11.38
		$K_D (mol^2 \cdot kJ^{-2})$	1.28×10 <sup>-5</sup> ±6.92×10 <sup>-5</sup>
		AIC	50.42
		$R^2$	0.43
Temkin	$q_e = \frac{RT}{b_T \ln A_T C_e}$	$b_T (J \cdot mol^{-1})$	380.98±69.24
		$A_T (L \cdot g^{-1})$	18.65±19.11
		AIC	41.91
		$R^2$	0.83

It is shown in Table 3 that the highest  $R^2$  value indicated that the adsorption isotherm of MTBE onto ZSM-5 fits the Sips model best which is a combination of the Langmuir and Freundlich isotherms. However, the Langmuir model has the lowest AIC value. In addition, the parameters of the Sips model generally depend on the operating conditions [27]. The Sips model reduces to Freundlich isotherm at low adsorbate concentrations, and predicts a monolayer adsorption capacity characteristic of Langmuir isotherm at high concentrations which is the condition of this study. Therefore, MTBE adsorption can be described best by

the Langmuir model, indicating a monolayer and homogeneous adsorption process. The maximum adsorption capacity is  $53.55 \text{ mg}\cdot\text{g}^{-1}$ , and the  $R_L$  value showed that the adsorption process is favorable.

According to the results obtained, ZSM-5 could be employed as an effective adsorbent for MTBE. Table 4 gives a comparison of the adsorption capacities of MTBE on different adsorbents obtained from the literature. The adsorption kinetics of MTBE onto all these adsorbents followed the pseudo-second-order model.

Table 4 Comparison of adsorption properties of MTBE with zeolites and other adsorbents

Adsorbents	Maximum adsorption capacity ( $\text{mg}\cdot\text{g}^{-1}$ )	Isotherm model	Reference
nano-PFOAL <sub>G</sub>	10.09	BET	[26]
nano-PFOAL <sub>B</sub>	10.41	BET	[26]
diatomite	-	Freundlich	[28]
mordenite	2.94	Freundlich	[29]
carbonaceous resin (Ambersorb 572)	4.97	Freundlich	[30]
lignite	0.13	Freundlich	[31]
activated carbon	66.72	Freundlich	[31]
activated carbon	1.94	Freundlich	[29]
HDTMA-modified clinoptilolite	91.60	Langmuir	[32]
Beta, Engelhard	25.06	Langmuir	[33]
ZSM-5	0.67	Langmuir	[33]
ZSM-5	95.00	Langmuir	[34,35]
ZSM-5	53.55	Langmuir	This study

nano-PFOAL: nano-perfluorooctyl alumina

### 3.3 Mass transfer mechanisms

#### 3.3.1 Transport progress in adsorption process

The mass transfer process has an impact on the adsorption equilibrium time. The mass transfer of adsorbate from the solution to the adsorption sites within the adsorbent particles is constrained by mass transfer resistances [17]. The mass transfer process generally involves four steps [36]: transport from the bulk solution to the boundary layer, film (boundary layer) diffusion, intra-particle (pore and surface) diffusion and adsorption on the interior surface of adsorbents. It is generally accepted that the first and last steps are very fast and the overall adsorption process is controlled by film diffusion and/or intra-particle diffusion [37].

#### 3.3.2 Film diffusion

Due to that the film diffusion influences only the beginning of the adsorption process, film mass transfer coefficients,  $k_f$  ( $\text{cm}\cdot\text{s}^{-1}$ ), were determined from the initial part of the kinetic curve ( $t=0$ ,  $c=c_0$ ,  $c_s=0$ ) [17] with the following equations:

$$k_f = - \frac{V_L}{a_m m_A c_0} \left( \frac{dc}{dt} \right)_{t=0}$$

$$a_m = \frac{3}{\rho_p r_p}$$

Where  $m_A$  is the adsorbent mass,  $V_L$  is the liquid volume,  $a_m$  is the total surface area related to the adsorbent mass,  $\rho_p$  is the density of adsorbent particles,  $r_p$  is the radius of adsorbent particles, and the value of  $r_p$  is  $2.5 \times 10^{-4}$  cm for ZSM-5 in this study,  $c_s$  is the concentration of MTBE at the external particle surface.  $\left( \frac{dc}{dt} \right)_{t=0}$  can be read from the slope of the tangent in the kinetic curve by setting  $t=0$ . The calculated  $k_f$  values decreased with the increasing MTBE concentrations ( $2.00 \times 10^{-5}$   $\text{cm}\cdot\text{s}^{-1}$  for 100 mg/L,  $1.34 \times 10^{-5}$   $\text{cm}\cdot\text{s}^{-1}$  for 150 mg/L,  $7.20 \times 10^{-6}$   $\text{cm}\cdot\text{s}^{-1}$  for 300 mg/L and  $3.96 \times 10^{-6}$   $\text{cm}\cdot\text{s}^{-1}$  for 600 mg/L).

### 3.3.3 Intra-particle diffusion

#### 3.3.3.1 Weber and Morris intra-particle diffusion model

After the film diffusion process, the adsorbate species are transported to the solid phase through intra-particle diffusion/transport process.

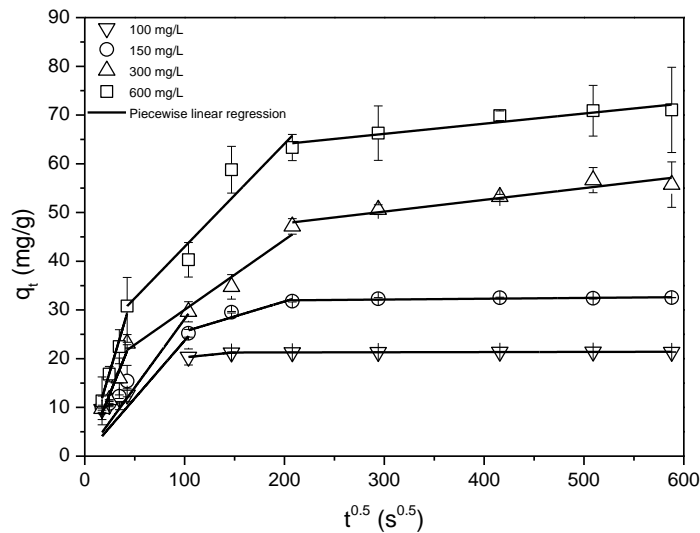


Figure 4 Intra-particle diffusion plot for MTBE adsorption onto ZSM-5 at initial MTBE concentration of 100, 150, 300 and 600 mg·L<sup>-1</sup>

Weber and Morris model was used to describe the process of intra-particle diffusion. The intra-particle diffusion rate constant,  $K_i$  (mg·g<sup>-1</sup>·s<sup>0.5</sup>), is defined by the following equation [38]:

$$q_t = K_i t^{0.5} + c$$

Where  $q_t$  is the amount of MTBE adsorbed (mg·g<sup>-1</sup>) at time  $t$ , and  $c$  is the intercept, giving the information about the thickness of boundary layer.

Figure 4 shows the intra-particle diffusion plot of MTBE adsorption on ZSM-5 and the piecewise linear regression results were presented in Table 5. From Figure 4, the plot of  $q_t$  against  $t^{0.5}$  showed three linear portions, indicating three periods involved in the sorption

process [39,40]. The first, sharper region describes the film diffusion. In this initial stage, ZSM-5 particles are surrounded by the boundary layer and MTBE molecules have to overcome the boundary layer resistance [41]. When the external surface of ZSM-5 reached saturation, MTBE entered the inner pores of ZSM-5 and was adsorbed onto the internal adsorption sites, i.e. the second stage where intra-particle diffusion happens. The slope of the second linear portion has been defined to yield the intra-particle diffusion parameter  $K_2$  ( $\text{mg}\cdot\text{g}^{-1}\cdot\text{s}^{-0.5}$ ) [39]. As shown in Table 5, the values of  $K_i$  increased with the increase of MTBE concentrations, indicating that the intra-particle diffusion rate increased with higher initial MTBE concentrations. The third region is the final equilibrium stage (after  $210 \text{ s}^{0.5}$ ) where intra-particle diffusion starts to slow down due to the extremely low adsorbate concentrations left in the solution [42].

Table 5 Piecewise linear regression parameters of intra-particle diffusion for MTBE onto ZSM-5

Parameters	Initial MTBE concentration ( $\text{mg}\cdot\text{L}^{-1}$ )			
	100	150	300	600
Intra-particle diffusion period	3-6 h	3-12 h	0.5-12 h	0.5-12 h
$K_2$ ( $\text{mg}\cdot\text{g}^{-1}\cdot\text{s}^{-0.5}$ )	0.02	$0.06\pm 0.02$	$0.14\pm 0.02$	$0.21\pm 0.04$
c	18.21	$19.43\pm 2.79$	$15.69\pm 2.52$	$21.81\pm 5.91$
$R^2$	1.00	0.85	0.95	0.89

It was shown in Figure 4 that all the curved plots covering the initial phase passed through the origin, suggesting that intra-particle diffusion should be the rate-controlling step in the removal of the adsorbate [40]. That is, film diffusion may be very fast and could be ignored [43]. To further judge whether the pore diffusion or surface diffusion was more important, the pore and surface diffusion coefficients were calculated as follows.



### 3.3.3.2 Pore diffusion

The pore diffusion coefficients largely depend on the surface properties of adsorbents. According to Bhattacharya and Venkobachar [44], the pore diffusion coefficient ( $D_p$ ) can be calculated with the pseudo-first-order kinetic model. Although MTBE adsorption on ZSM-5 followed the pseudo-second-order model, the  $R^2$  values ( $R^2 > 0.85$ ) of pseudo-first-order model were high enough. Therefore, this method is applicable to this study to estimate pore diffusion coefficients. The equation and obtained  $D_p$  values are shown in Table 6. The values of  $D_p$  for MTBE in the present study were found to be in the order of  $10^{-12}$ - $10^{-13}$   $\text{cm}^2 \cdot \text{s}^{-1}$  and decreased with the increasing MTBE concentrations.

### 3.3.3.3 Surface diffusion

The linear driving force model (LDF model), a simplification of the surface diffusion model, was used to estimate the surface mass transfer coefficient ( $k_s$ ,  $\text{cm} \cdot \text{s}^{-1}$ ) [45]. Furthermore, the values of  $D_s$ , the surface diffusion coefficient, are also calculated to compare with those of  $D_p$  to assess the rate-limiting step of the adsorption process. The equations and obtained values of  $D_s$  and  $k_s$  are shown in Table 6. Where  $A_s$  is the total external surface area of all adsorbent particles,  $q_s$  is the adsorbed amount at external particle surface which can be calculated from the adsorption isotherm,  $\bar{q}$  is the mean adsorbent loading.  $c_s(t)$  at time  $t$  can be read from the kinetic curve by setting  $c_s(t) = c(t)$  (fast film diffusion), and  $q_s(t)$  related to  $c_s(t)$  can be calculated by the isotherm equation. To find an average value for  $k_s$ , the procedure was repeated for different pairs of values ( $c$ ,  $t$ ).

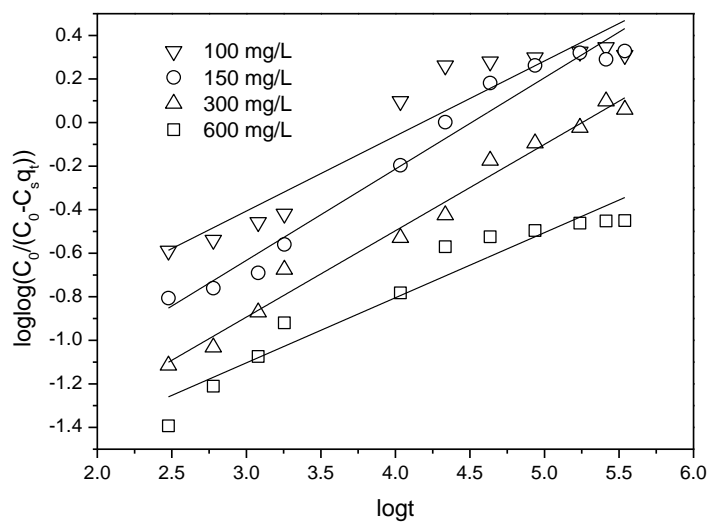
The values of  $D_s$  for MTBE in the present study were found to be in the order of  $10^{-13}$   $\text{cm}^2 \cdot \text{s}^{-1}$  and increased with the increase of MTBE concentration from Table 6. This may be due to that the increasing MTBE concentration increased the surface loading, thereby leading to an

1 increase of adsorbate mobility and a decrease of the adsorption energy [17]. This fell well  
 2 within the magnitudes for chemisorption system ( $10^{-5}$  to  $10^{-13}$   $\text{cm}^2 \cdot \text{s}^{-1}$ ) [46]. Since surface  
 3 diffusion and pore diffusion act in parallel and competitively, the faster process dominates  
 4 and determines the total adsorption rate. As a result, pore diffusion was the rate-limiting step  
 5 for MTBE adsorption on ZSM-5.  
 6  
 7  
 8  
 9  
 10

11  
 12  
 13  
 14 In addition, Bangham's equation was used for MTBE adsorption to test the role of diffusion  
 15 [47].  
 16

$$17 \log \log \left( \frac{C_0}{C_0 - C_s q_t} \right) = \log \left( \frac{K_b C_s}{2.303V} \right) + \alpha \log t$$

18  
 19  
 20  
 21  
 22  
 23 Where  $C_0$  is the initial MTBE concentration ( $\text{mg} \cdot \text{L}^{-1}$ ),  $C_s$  is the solid/liquid ratio ( $\text{g} \cdot \text{L}^{-1}$ ),  $q_t$  is  
 24 the amount of MTBE at time  $t$  ( $\text{mg} \cdot \text{g}^{-1}$ ),  $\alpha$  and  $K_b$  are constants.  $\log \log \left( \frac{C_0}{C_0 - C_s q_t} \right)$  was plotted  
 25 against  $\log t$  in Figure 5. The fitted linearity indicated the applicability of Bangham's model  
 26 ( $R^2 > 0.91$ ), and showed that the diffusion of MTBE into the pores of ZSM-5 mainly  
 27 controlled the adsorption process.  
 28  
 29  
 30  
 31  
 32  
 33  
 34  
 35  
 36  
 37  
 38



39  
 40  
 41  
 42  
 43  
 44  
 45  
 46  
 47  
 48  
 49  
 50  
 51  
 52  
 53  
 54  
 55  
 56  
 57 Figure 5 Bangham plot for MTBE adsorption on ZSM-5 at different initial concentrations  
 58  
 59  
 60  
 61  
 62  
 63  
 64  
 65

Table 6 Mass transfer and diffusion coefficients for MTBE adsorption on ZSM-5 at different initial concentrations

		Initial MTBE concentration (mg·L <sup>-1</sup> )			
		100	150	300	600
$D_p$ (cm <sup>2</sup> ·s <sup>-1</sup> )	$t_1 = \frac{0.03r_p^2}{D_p}$	42.88×10 <sup>-7</sup> 13	11.41×10 <sup>-7</sup> 13	8.97×10 <sup>-7</sup> 13	7.62×10 <sup>-7</sup> 13
$k_s$ (s <sup>-1</sup> )	$k_s = -\frac{k_f [c(t) - c_s(t)]}{\rho_p [q_s(t) - \bar{q}(t)]}$ $c_s(t) = c(t) + \frac{V_L}{m_A k_f a_m} \left(\frac{\partial c}{\partial t}\right)_t$ $A_s = a_m m_A = \frac{3m_A}{\rho_p r_p}$	5.15×10 <sup>-9</sup>	6.27×10 <sup>-9</sup>	12.97×10 <sup>-9</sup> 9	15.16×10 <sup>-9</sup> 9
$D_s$ (cm <sup>2</sup> ·s <sup>-1</sup> ) 1)	$D_s = \frac{k_s r_p}{5}$	2.57×10 <sup>-13</sup>	3.13×10 <sup>-13</sup>	6.49×10 <sup>-13</sup> 13	7.58×10 <sup>-13</sup> 13

### 3.4 Effect of initial solution pH

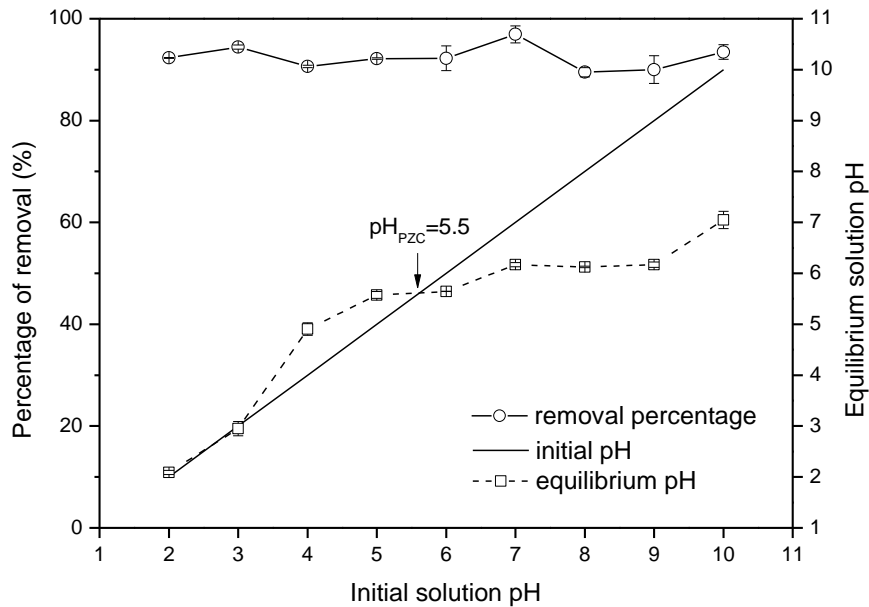


Figure 6 The effect of initial solution pH on the percentage of MTBE removal (the equilibrium solution pH is also presented)

1 Solution pH controls the electrostatic interactions between the adsorbent and adsorbate.  
 2 Therefore, it determines the adsorbent surface charge and the dissociation or protonation of  
 3 organic weak electrolytes [48]. As shown in Figure 6, the pH at PZC (point of zero charge) of  
 4 ZSM-5 was around 5.5. This means that when pH values were above 5.5, the surface of  
 5 ZSM-5 was negatively charged, which was favourable for cation exchange. It was also shown  
 6 that the removal percentage of MTBE onto ZSM-5 remained at ~90 % and was barely  
 7 affected by the change of initial solution pH. The same phenomenon was reported for the  
 8 adsorption of other organics [49,50]. This may be due to that ZSM-5 in this study has little  
 9 potential for the ion exchange considering its high SiO<sub>2</sub>/Al<sub>2</sub>O<sub>3</sub> ratio and low CEC (Cation  
 10 Exchange Capacity) value as shown in Table 1. In addition, MTBE is a weakly polar  
 11 molecule, and the protonation of the functional groups is not high enough to compete with the  
 12 sorption of water molecules due to the still strong H-bonding abilities of these groups  
 13 compared with their deprotonated counterparts [49], which leads to the weak electrostatic  
 14 interaction between ZSM-5 and MTBE.

### 3.5 Effect of solid to liquid ratio

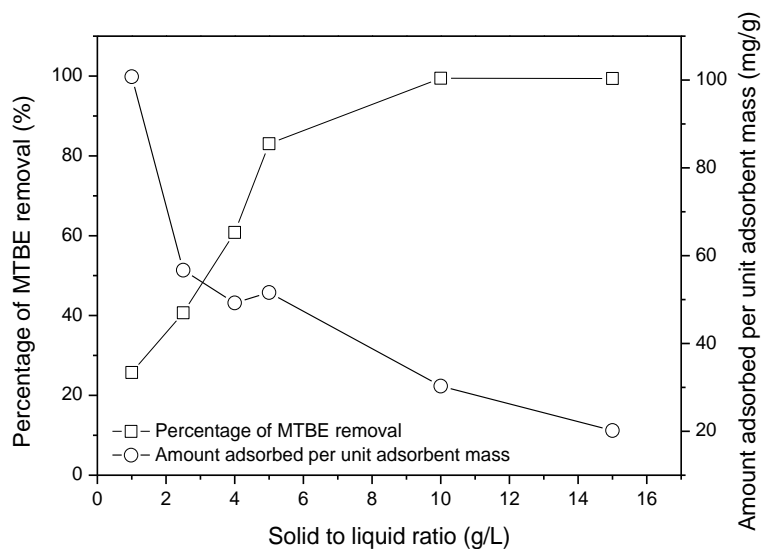


Figure 7 The effect of solid/liquid ratio on MTBE adsorption onto ZSM-5

As shown in Figure 7, the percentage of MTBE removal increased significantly from 25.73% to 99.42% with the increase of ZSM-5 dosage from 1 g·L<sup>-1</sup> to 10 g·L<sup>-1</sup> and remained constant beyond 10 g·L<sup>-1</sup>. The amount of MTBE adsorbed per unit adsorbent mass at equilibrium decreased across the ZSM-5 dosage range of 1-15 g·L<sup>-1</sup>.

### 3.6 Effect of the existence of Ni (II)

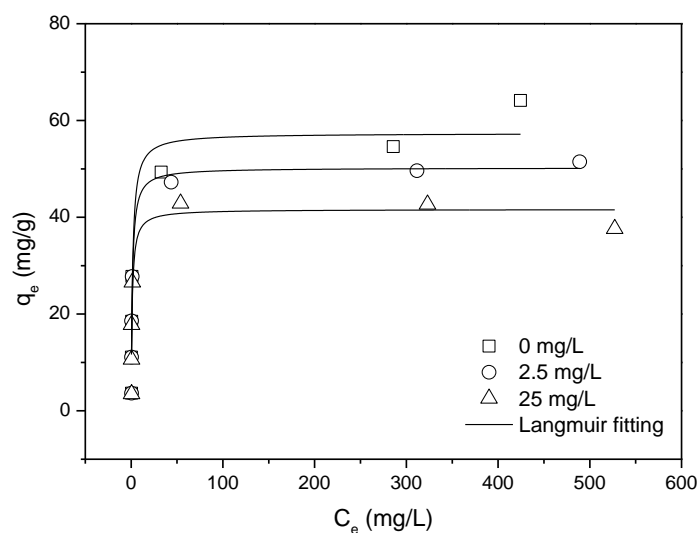


Figure 8 MTBE adsorption isotherms onto ZSM-5 with different concentrations of Ni (II) (0, 2.5 and 25 mg·L<sup>-1</sup>) (pH=7)

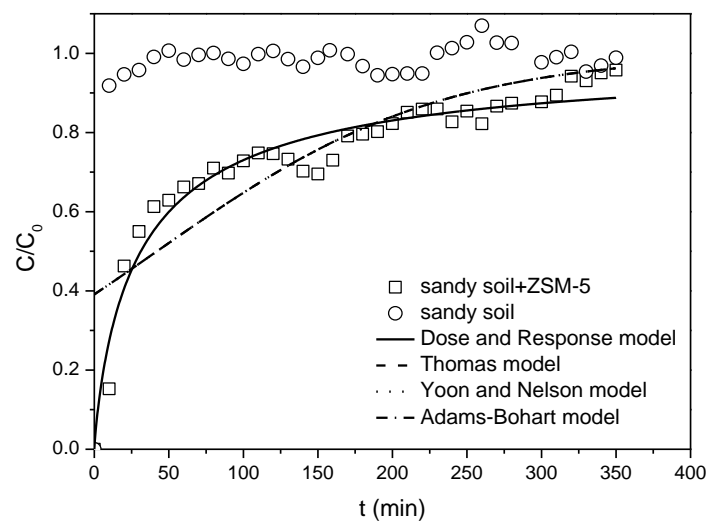
Effect of Ni(II) on the sorption of MTBE on ZSM-5 was evaluated in the presence of different concentrations of Ni<sup>2+</sup>. As shown in Figure 8, according to Langmuir model, the maximum adsorption capacities decreased with the increasing Ni<sup>2+</sup> concentrations (57.36 mg·g<sup>-1</sup> for 0 mg·L<sup>-1</sup> Ni<sup>2+</sup>, 50.22 mg·g<sup>-1</sup> for 2.5 mg·L<sup>-1</sup> Ni<sup>2+</sup> and 41.63 mg·g<sup>-1</sup> for 25 mg·L<sup>-1</sup> Ni<sup>2+</sup>, respectively). This indicated that the existence of Ni (II) had a suppression effect on MTBE adsorption onto ZSM-5. This may be attributed to both direct competition for sorption sites and pore blockage mechanism [49]. The surface complexation of hydrated Ni<sup>2+</sup> may

1 perturb surface chemistry and/or pore structure of ZSM-5. Similarly, the surface  
2 complexation of  $\text{Cu}^{2+}$  was also reported to have a suppression effect on the sorption of  
3 organics to wood charcoal [49]. In addition, considering the ionic radii of  $\text{Ni}^{2+}$  (0.7 Å),  
4 hydrated  $\text{Ni}^{2+}$  and thermochemical radii of  $\text{SO}_4^{2-}$  (2.58 Å), the addition of cations and anions  
5 and their hydrated products may lead to the increasing ionic strength and the occupation of  
6 the pores of ZSM-5. However, the detailed competitive adsorption mechanism between  $\text{Ni}^{2+}$   
7 (and other heavy metal contaminants) and MTBE is complex and warrants further studies.  
8  
9  
10  
11  
12  
13  
14  
15  
16  
17  
18

### 19 3.7 Desorption kinetics

20 The desorption characteristics are an important factor to evaluate the effectiveness of an  
21 adsorbent. The results showed that MTBE was hardly desorbed (<2%) after 96 h with initial  
22 MTBE concentration of  $300 \text{ mg}\cdot\text{L}^{-1}$ . This means that the adsorption between ZSM-5 and  
23 MTBE is very strong and ZSM-5 is an effective and suitable adsorbent for MTBE.  
24  
25  
26  
27  
28  
29  
30  
31  
32  
33

### 34 3.8 Fixed-bed column tests



35  
36  
37  
38  
39  
40  
41  
42  
43  
44  
45  
46  
47  
48  
49  
50  
51  
52  
53  
54  
55  
56  
57 Figure 9 The experimental and predicted breakthrough curves for the adsorption of  
58 MTBE on sand and sand-ZSM-5 mixture at an inlet MTBE concentration of  $300 \text{ mg}\cdot\text{L}^{-1}$   
59  
60  
61  
62  
63  
64  
65

1  
2 As the adsorption and desorption performance of ZSM-5 in batch adsorption studies was  
3  
4 good for MTBE removal, ZSM-5 was used as a reactive medium in fixed-bed column tests to  
5  
6 simulate its application in PRBs. Column tests were carried out with a total operational time  
7  
8 of 350 min to reach saturation in this study.  
9  
10

11  
12 From the breakthrough curves in Figure 9, the saturation time was about 320 min while the  
13  
14 control sample was saturated at the very beginning (within 10 minutes). This indicated that  
15  
16 sandy soil had almost no adsorption ability for MTBE and the addition of 5% ZSM-5 can  
17  
18 improve the removal performance significantly. The breakthrough time ( $C/C_0=0.5$ ) was about  
19  
20  
21  
22  
23  
24  
25  
26  
27  
28  
29  
30  
31  
32  
33  
34  
35  
36  
37  
38  
39  
40  
41  
42  
43  
44  
45  
46  
47  
48  
49  
50  
51  
52  
53  
54  
55  
56  
57  
58  
59  
60  
61  
62  
63  
64  
65

66  
67  
68  
69  
70  
71  
72  
73  
74  
75  
76  
77  
78  
79  
80  
81  
82  
83  
84  
85  
86  
87  
88  
89  
90  
91  
92  
93  
94  
95  
96  
97  
98  
99  
100  
101  
102  
103  
104  
105  
106  
107  
108  
109  
110  
111  
112  
113  
114  
115  
116  
117  
118  
119  
120  
121  
122  
123  
124  
125  
126  
127  
128  
129  
130  
131  
132  
133  
134  
135  
136  
137  
138  
139  
140  
141  
142  
143  
144  
145  
146  
147  
148  
149  
150  
151  
152  
153  
154  
155  
156  
157  
158  
159  
160  
161  
162  
163  
164  
165  
166  
167  
168  
169  
170  
171  
172  
173  
174  
175  
176  
177  
178  
179  
180  
181  
182  
183  
184  
185  
186  
187  
188  
189  
190  
191  
192  
193  
194  
195  
196  
197  
198  
199  
200  
201  
202  
203  
204  
205  
206  
207  
208  
209  
210  
211  
212  
213  
214  
215  
216  
217  
218  
219  
220  
221  
222  
223  
224  
225  
226  
227  
228  
229  
230  
231  
232  
233  
234  
235  
236  
237  
238  
239  
240  
241  
242  
243  
244  
245  
246  
247  
248  
249  
250  
251  
252  
253  
254  
255  
256  
257  
258  
259  
260  
261  
262  
263  
264  
265  
266  
267  
268  
269  
270  
271  
272  
273  
274  
275  
276  
277  
278  
279  
280  
281  
282  
283  
284  
285  
286  
287  
288  
289  
290  
291  
292  
293  
294  
295  
296  
297  
298  
299  
300  
301  
302  
303  
304  
305  
306  
307  
308  
309  
310  
311  
312  
313  
314  
315  
316  
317  
318  
319  
320  
321  
322  
323  
324  
325  
326  
327  
328  
329  
330  
331  
332  
333  
334  
335  
336  
337  
338  
339  
340  
341  
342  
343  
344  
345  
346  
347  
348  
349  
350  
351  
352  
353  
354  
355  
356  
357  
358  
359  
360  
361  
362  
363  
364  
365  
366  
367  
368  
369  
370  
371  
372  
373  
374  
375  
376  
377  
378  
379  
380  
381  
382  
383  
384  
385  
386  
387  
388  
389  
390  
391  
392  
393  
394  
395  
396  
397  
398  
399  
400  
401  
402  
403  
404  
405  
406  
407  
408  
409  
410  
411  
412  
413  
414  
415  
416  
417  
418  
419  
420  
421  
422  
423  
424  
425  
426  
427  
428  
429  
430  
431  
432  
433  
434  
435  
436  
437  
438  
439  
440  
441  
442  
443  
444  
445  
446  
447  
448  
449  
450  
451  
452  
453  
454  
455  
456  
457  
458  
459  
460  
461  
462  
463  
464  
465  
466  
467  
468  
469  
470  
471  
472  
473  
474  
475  
476  
477  
478  
479  
480  
481  
482  
483  
484  
485  
486  
487  
488  
489  
490  
491  
492  
493  
494  
495  
496  
497  
498  
499  
500  
501  
502  
503  
504  
505  
506  
507  
508  
509  
510  
511  
512  
513  
514  
515  
516  
517  
518  
519  
520  
521  
522  
523  
524  
525  
526  
527  
528  
529  
530  
531  
532  
533  
534  
535  
536  
537  
538  
539  
540  
541  
542  
543  
544  
545  
546  
547  
548  
549  
550  
551  
552  
553  
554  
555  
556  
557  
558  
559  
560  
561  
562  
563  
564  
565  
566  
567  
568  
569  
570  
571  
572  
573  
574  
575  
576  
577  
578  
579  
580  
581  
582  
583  
584  
585  
586  
587  
588  
589  
590  
591  
592  
593  
594  
595  
596  
597  
598  
599  
600  
601  
602  
603  
604  
605  
606  
607  
608  
609  
610  
611  
612  
613  
614  
615  
616  
617  
618  
619  
620  
621  
622  
623  
624  
625  
626  
627  
628  
629  
630  
631  
632  
633  
634  
635  
636  
637  
638  
639  
640  
641  
642  
643  
644  
645  
646  
647  
648  
649  
650  
651  
652  
653  
654  
655  
656  
657  
658  
659  
660  
661  
662  
663  
664  
665  
666  
667  
668  
669  
670  
671  
672  
673  
674  
675  
676  
677  
678  
679  
680  
681  
682  
683  
684  
685  
686  
687  
688  
689  
690  
691  
692  
693  
694  
695  
696  
697  
698  
699  
700  
701  
702  
703  
704  
705  
706  
707  
708  
709  
710  
711  
712  
713  
714  
715  
716  
717  
718  
719  
720  
721  
722  
723  
724  
725  
726  
727  
728  
729  
730  
731  
732  
733  
734  
735  
736  
737  
738  
739  
740  
741  
742  
743  
744  
745  
746  
747  
748  
749  
750  
751  
752  
753  
754  
755  
756  
757  
758  
759  
760  
761  
762  
763  
764  
765  
766  
767  
768  
769  
770  
771  
772  
773  
774  
775  
776  
777  
778  
779  
780  
781  
782  
783  
784  
785  
786  
787  
788  
789  
790  
791  
792  
793  
794  
795  
796  
797  
798  
799  
800  
801  
802  
803  
804  
805  
806  
807  
808  
809  
810  
811  
812  
813  
814  
815  
816  
817  
818  
819  
820  
821  
822  
823  
824  
825  
826  
827  
828  
829  
830  
831  
832  
833  
834  
835  
836  
837  
838  
839  
840  
841  
842  
843  
844  
845  
846  
847  
848  
849  
850  
851  
852  
853  
854  
855  
856  
857  
858  
859  
860  
861  
862  
863  
864  
865  
866  
867  
868  
869  
870  
871  
872  
873  
874  
875  
876  
877  
878  
879  
880  
881  
882  
883  
884  
885  
886  
887  
888  
889  
890  
891  
892  
893  
894  
895  
896  
897  
898  
899  
900  
901  
902  
903  
904  
905  
906  
907  
908  
909  
910  
911  
912  
913  
914  
915  
916  
917  
918  
919  
920  
921  
922  
923  
924  
925  
926  
927  
928  
929  
930  
931  
932  
933  
934  
935  
936  
937  
938  
939  
940  
941  
942  
943  
944  
945  
946  
947  
948  
949  
950  
951  
952  
953  
954  
955  
956  
957  
958  
959  
960  
961  
962  
963  
964  
965  
966  
967  
968  
969  
970  
971  
972  
973  
974  
975  
976  
977  
978  
979  
980  
981  
982  
983  
984  
985  
986  
987  
988  
989  
990  
991  
992  
993  
994  
995  
996  
997  
998  
999  
1000

the removal capacity was  $\sim 18.71 \text{ mg}\cdot\text{g}^{-1}$  and  $\sim 25\%$  MTBE was removed under the conditions of this study.

Table 7 Mathematic model parameters for the adsorption of MTBE onto ZSM-5 in fixed-bed column tests

Models	Equations	Parameters	
Adams-Bohart	$\frac{C}{C_i} = \frac{e^{k_{AB}C_i t}}{e^{(k_{AB}N_0 Z/v)} - 1 + e^{k_{AB}C_i t}}$	$k_{AB} (\text{L}\cdot\text{mg}^{-1}\cdot\text{min}^{-1})$ $N_0 (\text{mg}\cdot\text{L}^{-1})$ $R^2$	$3.51\times 10^{-5}\pm 4.67\times 10^{-6}$ $1902.84\pm 150.59$ $0.74$
Thomas	$\frac{C}{C_i} = \frac{1}{1 + e^{\frac{k_{Th}(q_0 m - C_i V)}{Q}}}$	$k_{Th} (\text{mL}\cdot\text{mg}^{-1}\cdot\text{min}^{-1})$ $q_0 (\text{mg}\cdot\text{g}^{-1})$ $R^2$ $q_{\text{total}} (\text{mg})$	$0.035\pm 0.005$ $9.00\pm 2.54$ $0.74$ $25.2$
Yoon and Nelson	$\frac{C}{C_i} = \frac{1}{1 + e^{k_{YN}(\tau - t)}}$	$k_{YN} (\text{min}^{-1})$ $\tau_{\text{cal}} (\text{min})$ $\tau_{\text{exp}} (\text{min})$ $R^2$	$0.011\pm 0.001$ $42.01\pm 11.83$ $25$ $0.74$
Dose-Response	$Y = \frac{C}{C_i} = 1 - \frac{1}{1 + (\frac{C_i V}{q_0 m})^a}$ $b = V_{(50\%)} = \frac{q_0 m}{C_i}$	$a$ $b$ $q_0 (\text{mg}\cdot\text{g}^{-1})$ $R^2$	$0.86\pm 0.05$ $0.062$ $6.69\pm 0.56$ $0.95$

#### 4. Conclusions

The detailed mass transfer mechanisms, adsorption and desorption features of ZSM-5 for MTBE removal were systematically discussed in this study. The conclusions are as follows.

- (1) Kinetics and isotherm studies indicate that ZSM-5 can be effectively employed for MTBE adsorption in both batch and column tests.
- (2) The adsorption follows the Langmuir model and obeys the pseudo-second-order model, suggesting a monolayer and homogeneous chemisorption process. 24 h is required to



1 reach adsorption equilibrium. MTBE is barely desorbed with the initial MTBE  
2 concentration of  $300 \text{ mg}\cdot\text{L}^{-1}$ .  
3

4  
5 (3) In terms of the mass transfer mechanisms, pore diffusion is the main rate-limiting step for  
6 the entire adsorption process, and film diffusion is very fast for MTBE concentrations  
7 from 100 to 600 mg/L.  
8

9  
10  
11 (4) The initial solution pH has little effect on the adsorption process in the pH range of 2-10,  
12 while the existence of nickel ions suppresses the adsorption of MTBE with Ni  
13 concentrations of  $2.5\text{-}25 \text{ mg}\cdot\text{L}^{-1}$ .  
14  
15  
16

17  
18  
19 (5) In the fixed-bed column tests, the breakthrough curve could be described by Dose-  
20 Response model and the saturation time is 320 min under the conditions of this study. The  
21 removal capacity is  $\sim 18.71 \text{ mg}\cdot\text{g}^{-1}$  with a flow rate of  $2 \text{ mL}\cdot\text{min}^{-1}$ . Therefore, ZSM-5 is a  
22 potential and effective reactive medium for MTBE removal in PRBs and further study  
23 will be conducted to assess the effect of different operational conditions in column tests.  
24  
25  
26  
27  
28  
29  
30  
31

### 32 33 34 **Acknowledgements**

35  
36 The authors are grateful to China Scholarship Council (CSC) for the financial help of the  
37 PhD studentship for the first author and to the Killam Trusts for providing the Izaak Walton  
38 Killam Memorial Postdoctoral Fellowship to the third author.  
39  
40  
41  
42  
43  
44  
45  
46  
47  
48  
49  
50  
51  
52  
53  
54  
55  
56  
57  
58  
59  
60  
61  
62  
63  
64  
65

## References

- [1] WHO, Methyl tertiary-Butyl Ether (MTBE) in drinkingwater, Background document for development of WHO guidelines for drinking-water quality, 2005.
- [2] US-EPA, O.o.U.S.T, Semiannual report of UST performance measures-End of fiscal year 2015 (October 1, 2014-September 30, 2015), Environmental Protection Agency, 2015.
- [3] P.S. Maravanki, E.G. Picco, G.I. Servetti, Riesgo de Contaminación Ambiental en SASH (Sistema de Almacenamiento Subterráneo de Hidrocarburos) asociado a la calidad de los controles en Argentina, in: 2º Simposio Argentino sobre Riesgo Ambiental, UTN, Córdoba, Argentina, 2011.
- [4] R.C. Pepino Minetti, H.R. Macaño, J. Britch, M.C. Allende, In situ chemical oxidation of BTEX and MTBE by ferrate: pH dependence and stability, *J. Hazard. Mater.* 324 (2017), 448-456.
- [5] E.R. Mancini, A. Steen, G.A. Rausina, D.C.L. Wong, W.R. Arnold, F.E. Gostomski, T. Davies, J.R. Hockett, W.A. Stubblefield, K.R. Drottar, T.A. Springer, P. Errico, MTBE ambient water quality criteria development: A public/private partnership, *Environ. Sci. Technol.* 36 (2) (2002) 125-129.
- [6] B.D. Lindsey, J.D. Ayotte, B.C. Jurgens, L.A. Desimone, Using groundwater age distributions to understand changes in methyl tert-butyl ether (MtBE) concentrations in ambient groundwater, Northeastern United States, *Sci. Total Environ.* 579 (2017) 579-587.
- [7] S. Mohebali, Degradation of methyl t-butyl ether (MTBE) by photochemical process in nanocrystalline TiO<sub>2</sub> slurry: mechanism, by-products and carbonate ion effect, *J. Environ. Chem. Eng.* 1(4) (2013) 1070-1078.
- [8] US EPA, Performance Assessment of a Permeable Reactive Barrier for Ground Water - Remediation Fifteen Years after Installation, Publication No. EPA/600/F-13/324, 2013.
- [9] O. Gibert, T. Rötting, J.L. Cortina, J. de Pablo, C. Ayora, J. Carrera, J. Bolzicco, In-situ remediation of acid mine drainage using a permeable reactive barrier in Aznalcollar (Sw Spain), *J. Haz. Mats.* 191(1) (2011) 287-295.

- 1  
2  
3  
4  
5  
6  
7  
8  
9  
10  
11  
12  
13  
14  
15  
16  
17  
18  
19  
20  
21  
22  
23  
24  
25  
26  
27  
28  
29  
30  
31  
32  
33  
34  
35  
36  
37  
38  
39  
40  
41  
42  
43  
44  
45  
46  
47  
48  
49  
50  
51  
52  
53  
54  
55  
56  
57  
58  
59  
60  
61  
62  
63  
64  
65
- [10] M.A. Anderson, Removal of MTBE and other organic contaminants from water by sorption to high silica zeolites, *Environ. Sci. Technol.* 34(4) (2000) 725-727.
- [11] I. Levchuk, A. Bhatnagar, M. Sillanpää, Overview of technologies for removal of methyl tert-butyl ether (MTBE) from water, *Sci. Total Environ.* 476 (2014) 415-433.
- [12] T.M. Statham, S.C. Stark, I. Snape, G.W. Stevens, K.A. Mumford, A permeable reactive barrier (PRB) media sequence for the remediation of heavy metal and hydrocarbon contaminated water: A field assessment at Casey Station, Antarctica, *Chemosphere*. 147 (2016) 368-375.
- [13] G. Neupane, R.J. Donahoe, Attenuation of trace elements in coal fly ash leachates by surfactant-modified zeolite, *J. Haz. Mats.* 229 (2012) 201-208.
- [14] R. Vignola, U. Cova, F. Fabiani, G. Grillo, M. Molinari, R. Sbardellati, R. Sisto, Remediation of hydrocarbon contaminants in groundwater using specific zeolites in full-scale pump&treat and demonstrative permeable barrier tests, *Stud. Surf. Sci. Catal.* 174 (2008) 573-576.
- [15] R. Vignola, R. Bagatin, D. Alessandra De Folly, C. Flego, M. Nalli, D. Ghisletti, R. Sisto, Zeolites in a permeable reactive barrier (PRB): One year of field experience in a refinery groundwater—Part 1: The performances, *Chem. Eng. J.* 178 (2011) 204-209.
- [16] A.A. Faisal, Z.A. Hmood, Groundwater protection from cadmium contamination by zeolite permeable reactive barrier, *Desalin Water Treat.* 53(5) (2015) 1377-1386.
- [17] E. Worch, Adsorption technology in water treatment: fundamentals, processes, and modeling, Walter de Gruyter, 2012.
- [18] A. Dyer, An introduction to zeolite molecular sieves, Australia: John Wiley & Sons, 1988.
- [19] S. Hong, H. Zhang, C.M. Duttweiler, A.T. Lemley, Degradation of methyl tertiary-butyl ether (MTBE) by anodic Fenton treatment, *J. Hazard. Mater.* 144 (2007), 29-40.

- 1  
2  
3  
4  
5  
6  
7  
8  
9  
10  
11  
12  
13  
14  
15  
16  
17  
18  
19  
20  
21  
22  
23  
24  
25  
26  
27  
28  
29  
30  
31  
32  
33  
34  
35  
36  
37  
38  
39  
40  
41  
42  
43  
44  
45  
46  
47  
48  
49  
50  
51  
52  
53  
54  
55  
56  
57  
58  
59  
60  
61  
62  
63  
64  
65
- [20] B.J. Cosby, G.M. Hornberger, R.B. Clapp, T. Ginn, A statistical exploration of the relationships of soil moisture characteristics to the physical properties of soils, *Water Resour. Res.* 20(6) (1984) 682-690.
- [21] M. Calero, F. Hernáinz, G. Blázquez, G. Tenorio, M.A. Martín-Lara, Study of Cr (III) biosorption in a fixed-bed column, *J. Haz. Mats.* 171(1) (2009) 886-893.
- [22] M.S.M. Chan, R.J. Lynch, Photocatalytic degradation of aqueous methyl-tert-butyl-ether (MTBE) in a supported-catalyst reactor, *Environ. Chem. Lett.* 1 (2003), 157-160.
- [23] Z. Shen, F. Jin, F. Wang, O. McMillan, A. Al-Tabbaa, Sorption of lead by Salisbury biochar produced from British broadleaf hardwood, *Bioresour. Technol.* 193 (2015) 553-556.
- [24] W.J. Weber, J.C. Morris, Kinetics of adsorption on carbon from solution, *J. Sanit. Eng. Div.* 89(2) (1963) 31-60.
- [25] A. Ebadi, J.S.S. Mohammadzadeh, A. Khudiev, What is the correct form of BET isotherm for modeling liquid phase adsorption? *Adsorption.* 15(1) (2009) 65-73.
- [26] A. Mirzaei, A. Ebadi, P. Khajavi, Kinetic and equilibrium modeling of single and binary adsorption of methyl tert-butyl ether (MTBE) and tert-butyl alcohol (TBA) onto nano-perfluorooctyl alumina, *Chem. Eng. J.* 231 (2013) 550-560.
- [27] A.B. Pérez-Marín, V.M. Zapata, J.F. Ortuno, M. Aguilar, J. Sáez, M. Lloréns, Removal of cadmium from aqueous solutions by adsorption onto orange waste, *J. Haz. Mats.* 139(1) (2007) 122-131.
- [28] M. Aivalioti, I. Vamvasakis, E. Gidarakos, BTEX and MTBE adsorption onto raw and thermally modified diatomite, *J. Haz. Mats.* 178(1) (2010) 136-143.
- [29] H.W. Hung, T.F. Lin, C. Baus, F. Sacher, H.J. Brauch, Competitive and hindering effects of natural organic matter on the adsorption of MTBE onto activated carbons and zeolites, *Environ. Technol.* 26(12) (2005) 1371-1382.

- 1  
2  
3  
4  
5  
6  
7  
8  
9  
10  
11  
12  
13  
14  
15  
16  
17  
18  
19  
20  
21  
22  
23  
24  
25  
26  
27  
28  
29  
30  
31  
32  
33  
34  
35  
36  
37  
38  
39  
40  
41  
42  
43  
44  
45  
46  
47  
48  
49  
50  
51  
52  
53  
54  
55  
56  
57  
58  
59  
60  
61  
62  
63  
64  
65
- [30] H.W. Hung, T.F. Lin, Adsorption of MTBE from contaminated water by carbonaceous resins and mordenite zeolite, *J. Haz. Mats.* 135(1) (2006) 210-217.
- [31] M. Aivalioti, D. Pothoulaki, P. Papoulias, E. Gidarakos, Removal of BTEX, MTBE and TAME from aqueous solutions by adsorption onto raw and thermally treated lignite, *J. Haz. Mats.* 207 (2012) 136-146.
- [32] S.K. Ghadiri, R. Nabizadeh, A.H. Mahvi, S. Nasser, H. Kazemian, A.R. Mesdaghinia, S. Nazmara, Methyl tert-butyl ether adsorption on surfactant modified natural zeolites, *Iranian J. Environ. Health. Sci. Eng.* 7(3) (2010) 241-252.
- [33] L. Abu-Lail, J.A. Bergendahl, R.W. Thompson, Adsorption of methyl tertiary butyl ether on granular zeolites: Batch and column studies, *J. Hazard. Mater.* 178 (2010), 363-369.
- [34] A. Martucci, I. Braschi, C. Bisio, E. Sarti, E. Rodeghero, R. Bagatin, L. Pasti, Influence of water on the retention of methyl tertiary-butyl ether by high silica ZSM-5 and Y zeolites: A multidisciplinary study on the adsorption from liquid and gas phase, *RSC Adv.* 5 (2015), 86997-87006.
- [35] E. Rodeghero, L. Pasti, E. Sarti, G. Cruciani, R. Bagatin, A. Martucci, Temperature-induced desorption of methyl tert-butyl ether confined on ZSM-5: An in situ synchrotron XRD powder diffraction study, *Minerals* 7 (2017), 34.
- [36] W.J. Weber, Evolution of a technology, *J. Sanit. Eng. Div.* 110(5) (1984) 899-917.
- [37] S. Mahdavi, N. Amini, The role of bare and modified nano nickel oxide as efficient adsorbents for the removal of  $Cd^{2+}$ ,  $Cu^{2+}$ , and  $Ni^{2+}$  from aqueous solution, *Environ. Earth Sci.* 75(23) (2016) 1468-1482.
- [38] T. Furusawa, J.M. Smith, Intra-particle mass transport in slurries by dynamic adsorption studies, *AIChE J.* 20(1) (1974) 88-93.

- 1  
2  
3  
4  
5  
6  
7  
8  
9  
10  
11  
12  
13  
14  
15  
16  
17  
18  
19  
20  
21  
22  
23  
24  
25  
26  
27  
28  
29  
30  
31  
32  
33  
34  
35  
36  
37  
38  
39  
40  
41  
42  
43  
44  
45  
46  
47  
48  
49  
50  
51  
52  
53  
54  
55  
56  
57  
58  
59  
60  
61  
62  
63  
64  
65
- [39] M.H. Kalavathy, T. Karthikeyan, S. Rajgopal, L.R. Miranda, Kinetic and isotherm studies of Cu (II) adsorption onto H<sub>3</sub>PO<sub>4</sub>-activated rubber wood sawdust, *J. Colloid Interface Sci.* 292(2) (2005) 354-362.
- [40] B.H. Hameed, M.I. El-Khaiary, Batch removal of malachite green from aqueous solutions by adsorption on oil palm trunk fibre: Equilibrium isotherms and kinetic studies, *J. Haz. Mats.* 154(1) (2008) 237-244.
- [41] G. McKay, M.S. Otterburn, J.A. Aga, Fuller's earth and fired clay as adsorbents for dyestuffs, *Water Air Soil Pollut.* 24(3) (1985) 307-322.
- [42] F.C. Wu, R.L. Tseng, R.S. Juang, Comparisons of porous and adsorption properties of carbons activated by steam and KOH, *J. Colloid Interface Sci.* 283(1) (2005) 49-56.
- [43] E. Tütem, R. Apak, C.F. Ünal, Adsorptive removal of chlorophenols from water by bituminous shale, *Water Res.* 32(8) (1998) 2315-2324.
- [44] A.K. Bhattacharya, C. Venkobachar, Removal of cadmium (II) by low cost adsorbents, *J. Environ. Eng.* 110(1) (1984) 110-122.
- [45] E. Glueckauf, Theory of chromatography, Part 10: Formulae for diffusion into spheres and their application to chromatography, *T. Faraday. Soc.* 51 (1955) 1540-1551.
- [46] B. Al Duri, G. McKay, Basic dye adsorption on carbon using a solid-phase diffusion model, *Chem. Eng. J.* 38(1) (1988) 23-31.
- [47] C. Aharoni, M. Ungarish, Kinetics of activated chemisorption. Part 2. Theoretical models. *J. Chem. Soc., Perkin Trans. 1*, 73 (1977) 456-464.
- [48] C. Moreno-Castilla, Adsorption of organic molecules from aqueous solutions on carbon materials, *Carbon.* 42(1) (2004) 83-94.
- [49] J. Chen, D. Zhu, C. Sun, Effect of heavy metals on the sorption of hydrophobic organic compounds to wood charcoal, *Environ. Sci. Technol.* 41(7) (2007) 2536-2541.

[50] D. Zhu, S. Hyun, J.J. Pignatello, L.S. Lee, Evidence for  $\pi$ - $\pi$  electron donor-acceptor interactions between  $\pi$ -donor aromatic compounds and  $\pi$ -acceptor sites in soil organic matter through pH effects on sorption, *Environ. Sci. Technol.* 38(16) (2004) 4361-4368.

1  
2  
3  
4  
5  
6  
7  
8  
9  
10  
11  
12  
13  
14  
15  
16  
17  
18  
19  
20  
21  
22  
23  
24  
25  
26  
27  
28  
29  
30  
31  
32  
33  
34  
35  
36  
37  
38  
39  
40  
41  
42  
43  
44  
45  
46  
47  
48  
49  
50  
51  
52  
53  
54  
55  
56  
57  
58  
59  
60  
61  
62  
63  
64  
65

Table 1 The physicochemical properties of ZSM-5

Surface area ( $\text{m}^2 \cdot \text{g}^{-1}$ )	Pore size ( $\text{\AA}$ )	Particle size ( $\mu\text{m}$ )	$\text{SiO}_2/\text{Al}_2\text{O}_3$	pH	CEC ( $\text{cmol} \cdot \text{kg}^{-1}$ )
400	5.3x5.6; 5.1x5.5	2-8	469	4.14	1.808



Table 2 Kinetics model parameters for MTBE adsorption onto ZSM-5 at different MTBE concentrations

Models	Equations	Parameters	Initial MTBE concentration (mg·L <sup>-1</sup> )			
			100	150	300	600
Pseudo-first-order	$q_t = q_e(1 - e^{-k_1 t})$	$q_e$ (mg·g <sup>-1</sup> )	21.35±0.10	32.40±0.20	49.55±2.94	67.29±2.40
		$k_1$ (h <sup>-1</sup> )	5.57±0.74	2.35±0.80	1.59±0.11	1.40±0.38
		AIC	43.59	51.04	50.95	29.98
		R <sup>2</sup>	0.94	0.84	0.95	0.92
Pseudo-second-order	$q_t = \frac{q_e^2 k_2 t}{1 + q_e k_2 t}$ $t_{\frac{1}{2}} = \frac{1}{k_2 q_e}$	$q_e$ (mg·g <sup>-1</sup> )	21.44±0.07	32.68±0.09	52.19±1.56	69.64±1.68
		$k_2$ (g·mg <sup>-1</sup> ·h <sup>-1</sup> )	0.38±0.04	0.067±0.01	0.03±0.00	0.021±0.00
		$t_{1/2}$ (s)	437.23	1644.07	2090.22	2461.75
		AIC	34.44	31.41	35.91	20.22
		R <sup>2</sup>	0.97	0.97	0.99	0.97

Table 3 Isotherm model parameters for MTBE adsorption on ZSM-5

Models	Equations	Parameters	
Langmuir	$q_e = \frac{Q_0 b C_e}{1 + b C_e}$ $R_L = \frac{1}{1 + b C_0}$	$Q_0$ (mg·g <sup>-1</sup> )	53.55±4.07
		$b$ (L·mg <sup>-1</sup> )	0.62±0.20
		$R_L$	0.002
		AIC	38.34
		$R^2$	0.90
Freundlich	$q_e = C_e^{\frac{1}{n}} K_F$	$K_F$ (mg·g <sup>-1</sup> )	19.60±4.91
		1/n	0.18±0.65
		AIC	44.53
		$R^2$	0.76
BET	$q_e = q_m \frac{K_B C_e}{(1 - K_L C_e)(1 - K_L C_e + K_B C_e)}$	$q_m$ (mg·g <sup>-1</sup> )	53.42±8.61
		$K_L$ (L·mg <sup>-1</sup> )	8.35×10 <sup>-6</sup> ±4.66×10 <sup>-4</sup>
		$K_B$ (L·mg <sup>-1</sup> )	0.62±0.27
		AIC	52.34
		$R^2$	0.87
Sips	$q_e = Q_0 \frac{K_S C_e^{\frac{1}{n}}}{1 + K_S C_e^{\frac{1}{n}}}$	$K_S$ (L·mg <sup>-1</sup> )	2.57±1.48
		$Q_0$ (mg·g <sup>-1</sup> )	52.39±2.62
		$N$	0.21±0.07
		AIC	45.27
		$R^2$	0.95
Dubinin-Radushkevich	$q_e = q_m \exp \left( -K_D \left( RT \ln \left( 1 + \frac{1}{C_e} \right) \right)^2 \right)$	$q_m$ (mg·g <sup>-1</sup> )	53.64±11.38
		$K_D$ (mol <sup>2</sup> ·kJ <sup>-2</sup> )	1.28×10 <sup>-5</sup> ±6.92×10 <sup>-5</sup>
		AIC	50.42
		$R^2$	0.43
Temkin	$q_e = \frac{RT}{b_T \ln A_T C_e}$	$b_T$ (J·mol <sup>-1</sup> )	380.98±69.24
		$A_T$ (L·g <sup>-1</sup> )	18.65±19.11
		AIC	41.91
		$R^2$	0.83

Table 4 Comparison of adsorption properties of MTBE with zeolites and other adsorbents

Adsorbents	Maximum adsorption capacity (mg·g <sup>-1</sup> )	Isotherm model	Reference
nano-PFOAL <sub>G</sub>	10.09	BET	[26]
nano-PFOAL <sub>B</sub>	10.41	BET	[26]
diatomite	-	Freundlich	[28]
mordenite	2.94	Freundlich	[29]
carbonaceous resin (Ambersorb 572)	4.97	Freundlich	[30]
lignite	0.13	Freundlich	[31]
activated carbon	66.72	Freundlich	[31]
activated carbon	1.94	Freundlich	[29]
HDTMA-modified clinoptilolite	91.60	Langmuir	[32]
Beta, Engelhard	25.06	Langmuir	[33]
ZSM-5	0.67	Langmuir	[33]
ZSM-5	95.00	Langmuir	[34,35]
ZSM-5	53.55	Langmuir	This study

nano-PFOAL: nano-perfluorooctyl alumina

Table 5 Piecewise linear regression parameters of intra-particle diffusion for MTBE onto  
ZSM-5

Parameters	Initial MTBE concentration ( $\text{mg}\cdot\text{L}^{-1}$ )			
	100	150	300	600
Intra-particle diffusion period	3-6 h	3-12 h	0.5-12 h	0.5-12 h
$K_2$ ( $\text{mg}\cdot\text{g}^{-1}\cdot\text{s}^{-0.5}$ )	0.02	$0.06\pm 0.02$	$0.14\pm 0.02$	$0.21\pm 0.04$
c	18.21	$19.43\pm 2.79$	$15.69\pm 2.52$	$21.81\pm 5.91$
$R^2$	1.00	0.85	0.95	0.89

Table 6 Mass transfer and diffusion coefficients for MTBE adsorption on ZSM-5 at different initial concentrations

		Initial MTBE concentration (mg·L <sup>-1</sup> )			
		100	150	300	600
$D_p$ (cm <sup>2</sup> ·s <sup>-1</sup> )	$t_{\frac{1}{2}} = \frac{0.03r_p^2}{D_p}$	42.88×10 <sup>-13</sup>	11.41×10 <sup>-13</sup>	8.97×10 <sup>-13</sup>	7.62×10 <sup>-13</sup>
1)		13	13		
$k_s$ (s <sup>-1</sup> )	$k_s = -\frac{k_f [c(t) - c_s(t)]}{\rho_p [q_s(t) - \bar{q}(t)]}$ $c_s(t) = c(t) + \frac{V_L}{m_A k_f a_m} \left(\frac{\partial c}{\partial t}\right)_t$ $A_s = a_m m_A = \frac{3m_A}{\rho_p r_p}$	5.15×10 <sup>-9</sup>	6.27×10 <sup>-9</sup>	12.97×10 <sup>-9</sup>	15.16×10 <sup>-9</sup>
1)	$D_s = \frac{k_s r_p}{5}$	2.57×10 <sup>-13</sup>	3.13×10 <sup>-13</sup>	6.49×10 <sup>-13</sup>	7.58×10 <sup>-13</sup>

Table 7 Mathematic model parameters for the adsorption of MTBE onto ZSM-5 in fixed-bed column tests

Models	Equations	Parameters	
Adams-Bohart	$\frac{C}{C_i} = \frac{e^{k_{AB}C_i t}}{e^{(k_{AB}N_0Z/v)} - 1 + e^{k_{AB}C_i t}}$	$k_{AB}$ (L·mg <sup>-1</sup> ·min <sup>-1</sup> )	$3.51 \times 10^{-5} \pm 4.67 \times 10^{-6}$
		$N_0$ (mg·L <sup>-1</sup> )	$1902.84 \pm 150.59$
		$R^2$	0.74
Thomas	$\frac{C}{C_i} = \frac{1}{1 + e^{\frac{k_{Th}}{Q}(q_0 m - C_i V)}}$	$k_{Th}$ (mL·mg <sup>-1</sup> ·min <sup>-1</sup> )	$0.035 \pm 0.005$
		$q_0$ (mg·g <sup>-1</sup> )	$9.00 \pm 2.54$
		$R^2$	0.74
		$q_{total}$ (mg)	25.2
Yoon and Nelson	$\frac{C}{C_i} = \frac{1}{1 + e^{k_{YN}(\tau - t)}}$	$k_{YN}$ (min <sup>-1</sup> )	$0.011 \pm 0.001$
		$\tau_{cal}$ (min)	$42.01 \pm 11.83$
		$\tau_{exp}$ (min)	25
		$R^2$	0.74
Dose-Response	$Y = \frac{C}{C_i} = 1 - \frac{1}{1 + (\frac{C_i V}{q_0 m})^a}$	a	$0.86 \pm 0.05$
		b	0.062
		$q_0$ (mg·g <sup>-1</sup> )	$6.69 \pm 0.56$
	$b = V_{(50\%)} = \frac{q_0 m}{C_i}$	$R^2$	0.95

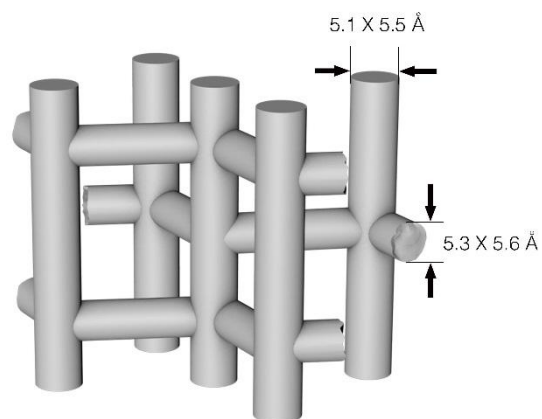


Figure 1 Molecular structure and dimensions of ZSM-5 [18]

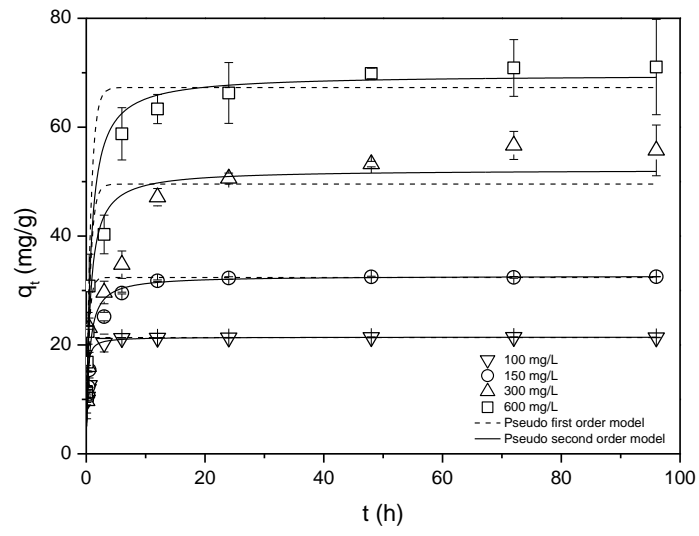


Figure 2 The fitting of pseudo-first-order and pseudo-second-order models for MTBE adsorption onto ZSM-5 at different initial concentrations



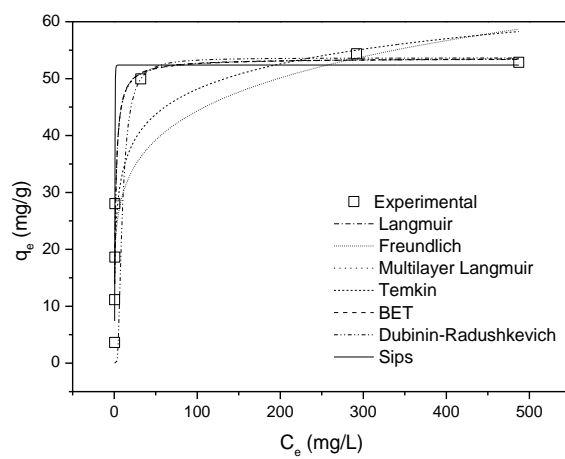


Figure 3 Isotherm plots for MTBE adsorption onto ZSM-5

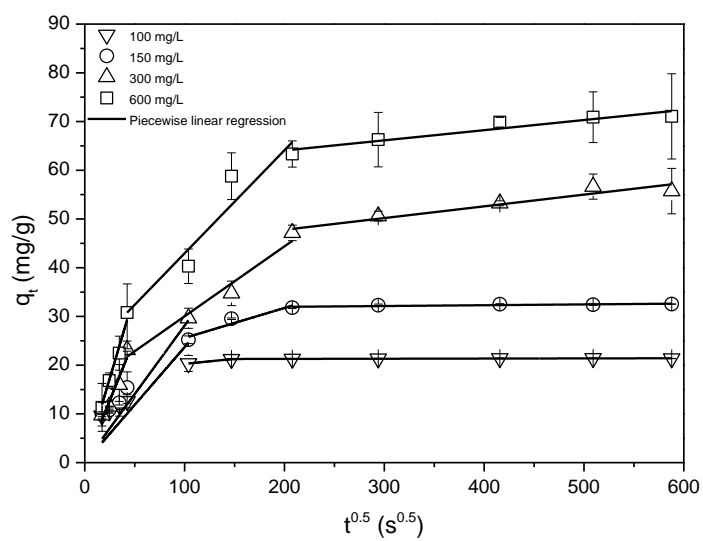


Figure 4 Intra-particle diffusion plot for MTBE adsorption onto ZSM-5 at initial MTBE concentration of 100, 150, 300 and 600  $\text{mg}\cdot\text{L}^{-1}$

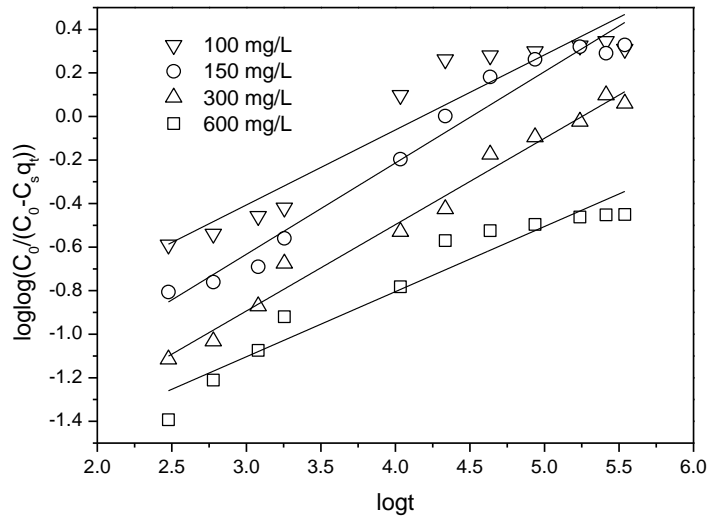


Figure 5 Bangham plot for MTBE adsorption on ZSM-5 at different initial concentrations

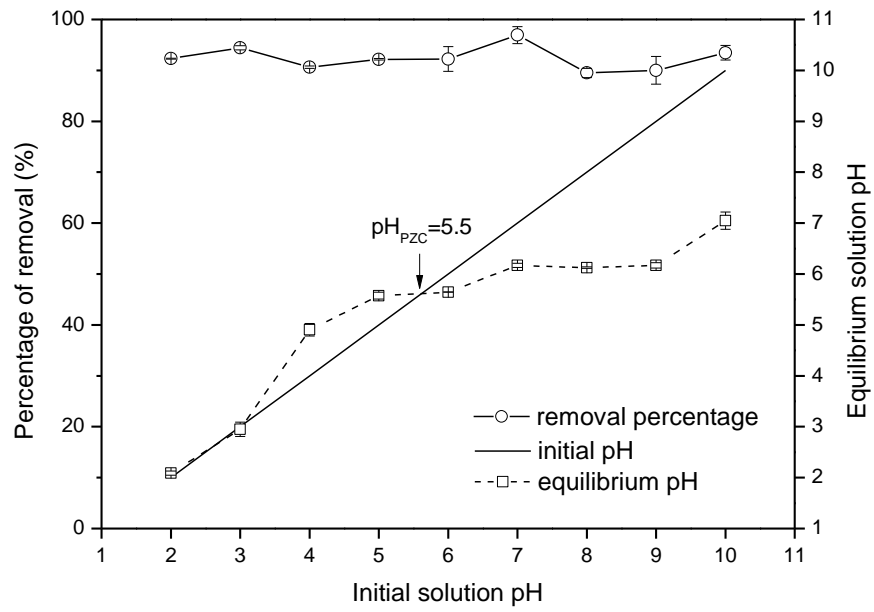


Figure 6 The effect of initial solution pH on the percentage of MTBE removal (the equilibrium solution pH is also presented)

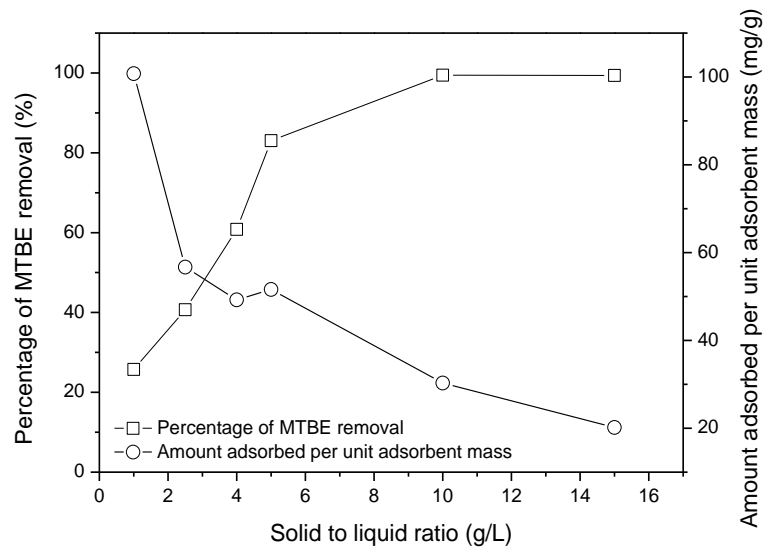


Figure 7 The effect of solid/liquid ratio on MTBE adsorption onto ZSM-5

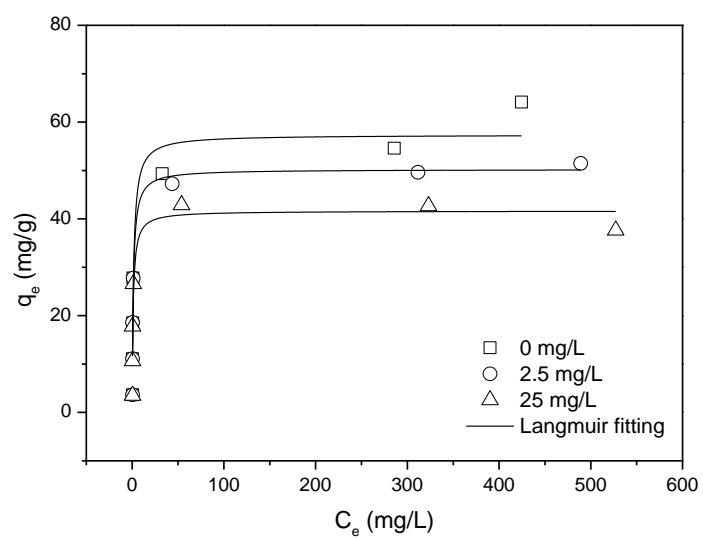


Figure 8 MTBE adsorption isotherms onto ZSM-5 with different concentrations of Ni (II) (0, 2.5 and 25 mg·L<sup>-1</sup>) (pH=7)

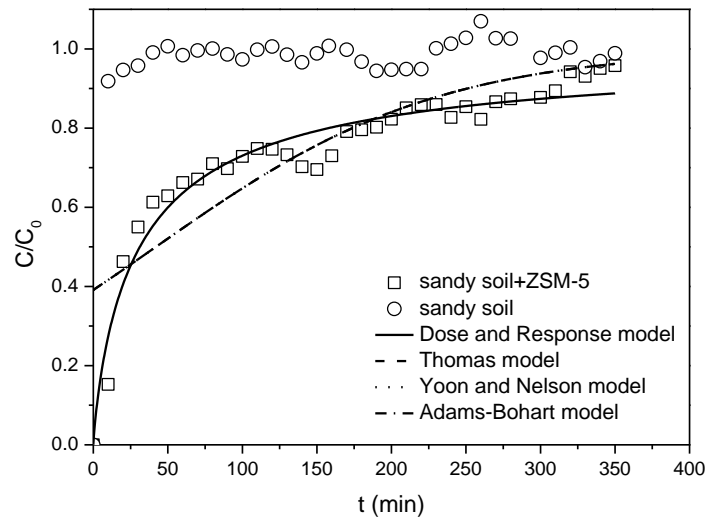


Figure 9 The experimental and predicted breakthrough curves for the adsorption of MTBE on sand and sand-ZSM-5 mixture at an inlet MTBE concentration of  $300 \text{ mg}\cdot\text{L}^{-1}$

## Highlights

1. The adsorption process of MTBE on ZSM-5 was explored with batch and column tests.
2. The adsorption follows the Langmuir model and obeys a pseudo-second-order model.
3. Pore diffusion is the main rate-limiting step for the entire adsorption process.
4. pH has little effect, while nickel ions suppress the adsorption process.
5. The removal capacity is  $\sim 18.71 \text{ mg}\cdot\text{g}^{-1}$  in fixed-bed column tests.



## Novelty Statement

ZSM-5 has significant potential as the reactive medium in PRBs for MTBE polluted groundwater remediation due to high and strong adsorption capacity. However, there is a lack of research into detailed mass transfer mechanisms and adsorption process, which is crucial for designing adsorption systems. This study explores the mass transfer and adsorption process in detail considering the effect of pH, co-existence of heavy metals, solid/liquid ratio and MTBE concentration. Additionally, the breakthrough curve of fixed-bed column tests was obtained and modelled. The results would offer considerable insights into the applicability of ZSM-5 in PRBs for environmental remediation.